

Two-photon absorption and emission by Rydberg atoms in coupled cavities

Huaizhi Wu,^{*} Zhen-Biao Yang,[†] and Shi-Biao Zheng

Department of Physics, Fuzhou University, Fuzhou 350002, People's Republic of China

We study the dynamics of a system composed of two coupled cavities, each interacting with a single Rydberg atom. The interplay between Rydberg-Rydberg interaction and photon hopping enables the transition of the atoms from the collective ground state to the double Rydberg excitation state by individually interacting with the optical normal modes and suppressing the up conversion process between them. The atomic transition is accompanied by the two-photon absorption and emission of the normal modes. Since the energy level structure of the atom-cavity system is photon number dependent there is only a pair of states being in the two-photon resonance. Therefore, the system can act as a quantum nonlinear absorption filter through the nonclassical quantum process, converting coherent light field into a non-classical state. Meanwhile, the vacuum field in the cavity inspires the Rydberg atoms to simultaneously emit two photons into the normal mode, resulting in obvious emission enhancement of the mode.

PACS numbers: 42.50.Pq, 32.80.Qk, 32.80.Ee

I. INTRODUCTION

The generation of nonclassical states of light has been a central topic in quantum optics since the first demonstration of squeezed states of light [1]. Quantum field in nonclassical states reveals their nonclassical properties by exhibiting photon anti-bunching, sub-Poisson photon-number statistics, and clearly negative values of the Wigner function [2]. These states can be used for understanding of quantum fluctuations beyond the standard quantum noise limit and are essential sources in optical science and engineering [3]. In this context, the two-photon process, namely, the atoms transit from one energy level to another through an intermediate energy level that simultaneously involves two photons of the same frequency (the degenerate two-photon transition) or of different frequencies (the nondegenerate two-photon transition), has attracted great interest because it provides great opportunity for producing light with nonclassical properties [4]. Indeed, the two-photon absorption and emission are inherently nonclassical effects, which are expected to have potential applications in the realm of quantum techniques [5–7].

Recently, high-finesse optical cavity has been used to couple Rydberg atoms with quantized cavity modes, which presents potential applications in studying photon nonlinearity and many-body physics [8–10]. Neutral atoms excited by laser beams and the cavity field to high-lying Rydberg states can interact through strong and long-range dipole-dipole or van der Waals interaction [11]. The quantum anharmonicity of the energy level structure of the atom-cavity system enables the study of two-photon absorption and three-photon absorption from a probe beam [8]. The optical nonlinearity has been experimentally explored with strongly interacting Rydberg atoms in cavities [12], even at the level of individual

quanta [13]. Moreover, Zhang et al. have shown that coupling of optical cavity to a lattice of Rydberg atoms can be described by the Dicke model, the competition between the atom-atom interaction and atom-light coupling can induce a novel superradiant solid phase [9]. On the other hand, rich quantum dynamics has been found in the coupling of the coupled cavities with neutral atoms [14, 15]. Its potential applications include realization of paradigmatic many-body models, such as the Bose-Hubbard and the anisotropic Heisenberg models [16].

Combine coupled cavities with interacting Rydberg atoms, a physical model in analogous to the quantum dot-cavity coupling system, where the cavity mode can be tuned to resonantly drive the two-photon transition between the ground and the biexciton states, while the exciton states are far-off resonance due to the biexciton binding energy [17], will be discussed here. In the paper, we study the two-photon absorption and emission process with two Rydberg atoms separately trapped in coupled cavities. There exists two newly optical normal modes due to the photon hopping between the two cavities. The collectively excited energy level of the Rydberg atoms is shifted up or down according to the sign of the Förster defects, which induces the two-photon resonant atomic transitions for either normal modes. In result, the blockade of simultaneous excitation to the Rydberg state fails due to the photon dynamics. The resonant transition frequency between the collective ground state and the double Rydberg excitation state is photon number dependent, leading to varied two-photon absorption rate for different states of the cavity modes. The system can be used for realization of quantum nonclassical processes and preparation of two-photon states. The results are discussed in the context of micro-cavities, however, the phenomenon may be found in other hybrid systems, such as Rydberg atoms interacting with superconducting microwave devices [18, 19].

^{*} huaizhi.wu@fzu.edu.cn

[†] zbyang@fzu.edu.cn

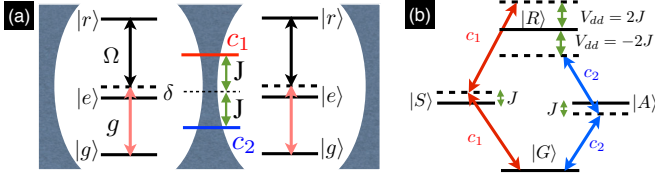


FIG. 1. (Color online) (a) Schematic setup: Two coupled cavities with each coupling to a single Rydberg atom. Coherent Rydberg excitation between $|g\rangle$ and $|r\rangle$ through a two-photon process via intermediate state $|e\rangle$. The quantized cavity fields are coupled to the blue of the $|g\rangle \leftrightarrow |e\rangle$ transition, and laser light is tuned to the red of the $|e\rangle \leftrightarrow |r\rangle$ transition. Photon hopping between the left and right cavity leads to two new delocalized normal modes c_1 and c_2 , with the bare frequency separated by $2J$. (b) Effective model for heralded two-photon transition between atomic collective states $|G\rangle$ and $|R\rangle$ through the intermediate symmetric and anti-symmetric entangled states $|S\rangle$ and $|A\rangle$. The c_1 mode is in two-photon resonance with the $|G\rangle \leftrightarrow |R\rangle$ transition for $V_{dd} = 2J$, while the c_2 mode is red detuned by $4J$. For $V_{dd} = -2J$, the situation is in reverse.

II. INTERACTING ATOMS IN COUPLED CAVITIES

Consider the system composed of two coupled cavities, each interacting with a Rubidium atom. This may be realized with micro-cavities (e.g. microtoroidal resonators), which can couple to each other via the overlap of their evanescent fields. The atoms have three relevant energy levels. As shown in Fig. 1, the transition from $5S_{1/2}$ atomic ground state denoted by $|g\rangle$ couples to a Rydberg excited level $|r\rangle$ through a two-photon process via the $5P_{3/2}$ intermediate state $|e\rangle$ [8]. The bare energies for the corresponding energy levels are $\hbar\omega_g$, $\hbar\omega_e$ and $\hbar\omega_r$, respectively. The atomic transitions $|g\rangle \leftrightarrow |e\rangle$ and $|e\rangle \leftrightarrow |r\rangle$ are coupled to quantized cavity field of frequency ω_c and laser field of frequency ω with Rabi frequency g and Ω , respectively. The cavity field is detuned by δ to the blue of the $|g\rangle \leftrightarrow |e\rangle$ transition, and laser beam is detuned by δ to the red of the $|e\rangle \leftrightarrow |r\rangle$ transition. The energy shift V_{dd} for the collective atomic state $|r\rangle_1|r\rangle_2$ stemming from the Rydberg-Rydberg interaction prevents the simultaneous excitation of the atoms to the Rydberg state $|r\rangle$. Photons can hop between the left and right cavities with the rate J , giving rise to a couple of optical normal modes with the frequencies $\omega_c \pm J$. The Hamiltonian for the coupled atom-cavity system in the rotating wave approximation (RWA) reads (assuming $\hbar = 1$)

$$H = H_c + H_a + H_{af}, \quad (1)$$

with

$$H_c = \omega_c(a_1^\dagger a_1 + a_2^\dagger a_2) + J(a_1^\dagger a_2 + a_1 a_2^\dagger),$$

$$H_a = \sum_{k=1,2} (\omega_g |g\rangle_{kk} \langle g| + \omega_e |e\rangle_{kk} \langle e| + \omega_r |r\rangle_{kk} \langle r|)$$

$$+ V_{dd} |r\rangle_1 |r\rangle_2 \langle r|_1 \langle r|,$$

and

$$H_{af} = \sum_{k=1,2} (g |e\rangle_{kk} \langle g| a_k + \Omega e^{-i\omega t} |r\rangle_{kk} \langle e|) + h.c.,$$

where a_k ($k = 1, 2$) are annihilation operators for cavity fields 1 and 2, respectively. We have assumed that the coupling strengths of the two atoms interacting with the respective local cavity modes and laser beams are real and identical for simplicity. In the large detuning regime, i.e., $\delta \gg \Omega, g$, the intermediate state $|e\rangle$ will not be populated and can be adiabatically eliminated. Thus, we have an effective Hamiltonian, which, in the interaction picture, is given by

$$H_I = H'_c + H'_a + H'_{af}, \quad (2)$$

with

$$H'_c = J(a_1^\dagger a_2 + a_1 a_2^\dagger),$$

$$H'_a = V_{dd} |r\rangle_1 |r\rangle_2 \langle r|_1 \langle r|,$$

and

$$H'_{af} = (\lambda \sum_{k=1,2} |r\rangle_{kk} \langle g| a_k + h.c.) + \lambda' \sum_{k=1,2} a_k^\dagger a_k |g\rangle_{kk} \langle g| + \lambda'' \sum_{k=1,2} |r\rangle_{kk} \langle r|,$$

where $\lambda = \Omega g / \delta$, $\lambda' = g^2 / \delta$, and $\lambda'' = \Omega^2 / \delta$.

For taking account of the Rydberg-Rydberg interaction between the atoms, it is convenient to rewrite the atom-cavity interaction in terms of the two-atom collective states $\{|G\rangle = |g\rangle_1 |g\rangle_2, |R\rangle = |r\rangle_1 |r\rangle_2, |S\rangle = (|g\rangle_1 |r\rangle_2 + |r\rangle_1 |g\rangle_2) / \sqrt{2}, |A\rangle = (|g\rangle_1 |r\rangle_2 - |r\rangle_1 |g\rangle_2) / \sqrt{2}\}$, and of the normal modes c_1 and c_2 , which are symmetric and antisymmetric superposition of the localized cavity annihilation operators,

$$c_1 = \frac{1}{\sqrt{2}}(a_1 + a_2),$$

$$c_2 = \frac{1}{\sqrt{2}}(a_1 - a_2). \quad (3)$$

Then, we have

$$H_I = H'_c + H'_a + H'_{af}, \quad (4)$$

with

$$H'_c = J(c_1^\dagger c_1 - c_2^\dagger c_2),$$

$$H'_a = V_{dd} |R\rangle \langle R|,$$

and

$$\begin{aligned}
H'_{af} = & [\lambda c_1(|S\rangle\langle G| + |R\rangle\langle S|) + \lambda c_2(|A\rangle\langle G| - |R\rangle\langle A|) \\
& + \frac{\lambda'}{2}(c_1^\dagger c_2 + c_2^\dagger c_1)|S\rangle\langle A| + h.c.] \\
& + \left(\frac{\lambda'}{2}(c_1^\dagger c_1 + c_2^\dagger c_2) + \lambda''\right)(|S\rangle\langle S| + |A\rangle\langle A|) \\
& + \lambda'(c_1^\dagger c_1 + c_2^\dagger c_2)|G\rangle\langle G| + 2\lambda''|R\rangle\langle R|.
\end{aligned}$$

The Hamiltonian H'_c represents the non-interacting delocalized modes with the frequency separated by $2J$. For the atom-field interaction Hamiltonian H'_{af} , the first four terms describe the atomic transitions from the collective ground state $|G\rangle$ to the double Rydberg excitation state $|R\rangle$ through two independent channels $|G\rangle \rightarrow |S\rangle \rightarrow |R\rangle$ and $|G\rangle \rightarrow |A\rangle \rightarrow |R\rangle$, by interacting individually with the normal modes c_1 and c_2 . The two transition channels link to each other via the optical frequency up conversion associated with the atomic transition $|S\rangle \leftrightarrow |A\rangle$, which is described by the fifth and sixth terms. The other terms are stark shifts for the related collective atomic states.

III. TWO-PHOTON COHERENT DYNAMICS AND RYDBERG BIEXCITATION

To gain the insight of the full dynamics, we finally pass to a new interaction Hamiltonian in a rotating frame with respect to $H'_c + H'_a = J(c_1^\dagger c_1 - c_2^\dagger c_2) + V_{dd}|R\rangle\langle R|$,

$$H'_I = H_{tr} + H_{st}, \quad (5)$$

with

$$\begin{aligned}
H_{tr} = & \lambda c_1 e^{-iJt}|S\rangle\langle G| + \lambda c_2 e^{iJt}|A\rangle\langle G| \\
& + \lambda c_1 e^{i(V_{dd}-J)t}|R\rangle\langle S| - \lambda c_2 e^{i(V_{dd}+J)t}|R\rangle\langle A| \\
& + \frac{\lambda'}{2}(c_1^\dagger c_2 e^{i2Jt} + c_2^\dagger c_1 e^{-i2Jt})|S\rangle\langle A| + h.c.,
\end{aligned}$$

and

$$\begin{aligned}
H_{st} = & \left(\frac{\lambda'}{2}(c_1^\dagger c_1 + c_2^\dagger c_2) + \lambda''\right)(|S\rangle\langle S| + |A\rangle\langle A|) \\
& + \lambda'(c_1^\dagger c_1 + c_2^\dagger c_2)|G\rangle\langle G| + 2\lambda''|R\rangle\langle R|.
\end{aligned}$$

(i) Without considering the photon number dependent stark shifts H_{st} . The normal mode c_1 is blue-detuned by J from the transition $|G\rangle \leftrightarrow |S\rangle$ and c_1 is red-detuned by J from the transition $|G\rangle \leftrightarrow |A\rangle$, see Fig. 1(b). To decouple the transition channels $|G\rangle \rightarrow |S\rangle \rightarrow |R\rangle$ and $|G\rangle \rightarrow |A\rangle \rightarrow |R\rangle$, the optical frequency up conversion should be suppressed. This can be met if the frequency separation of the normal modes is much greater than the conversion rate (dispersive regime), i.e., $2J \gg \sqrt{n_{c1}n_{c2}}\lambda'/2$. Note that the sign of the Rydberg-Rydberg interaction strength is determined by the sign of the energy gap in the Förster process [20]. Now if $V_{dd} = 2J$, the atomic transition $|G\rangle \leftrightarrow |R\rangle$ mediated by symmetric entangled state $|S\rangle$ is in resonance with twice the photon

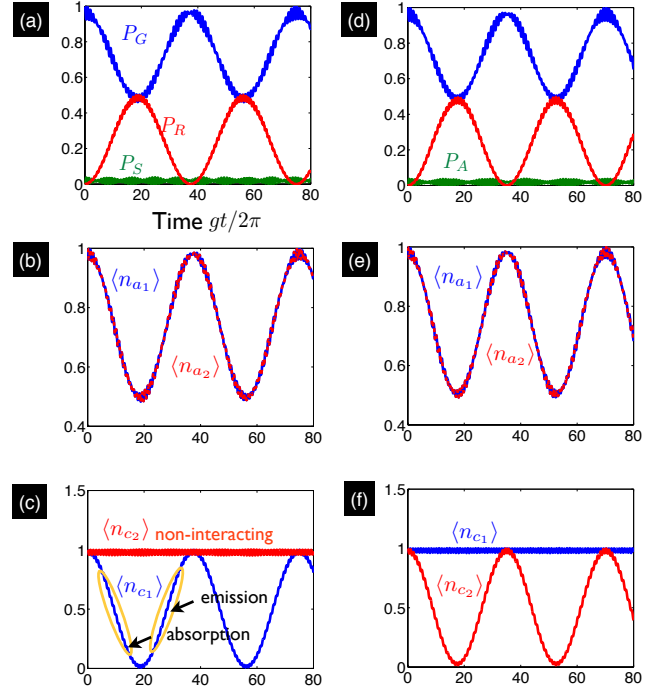


FIG. 2. (Color online) Time-dependent population of the collective atomic states, mean photon number for localized modes a_1 and a_2 , and mean photon number for delocalized normal modes c_1 and c_2 with the initial state $|G\rangle \otimes |1\rangle_{a1}|1\rangle_{a2}$. The parameters are $\Omega/g = 1$, $\delta = 10g$, $J = 10g$ with the Rydberg-Rydberg interaction strength $V_{dd} = 2J$ in (a)-(c) and $V_{dd} = -2J$ in (d)-(f). (a) and (d): Population of collective state P_G and P_R display sinusoidal oscillation due to the absorption and emission of two photons (see (b) and (e)). The photon dynamics for $\langle a_1 \rangle$ and $\langle a_2 \rangle$ are identical, while the dynamics of the delocalized modes c_1 and c_2 exhibit symmetric breaking. (c): For $V_{dd} = 2J$, the absorption of two photons from c_1 leads to atomic transition $|G\rangle \otimes |2\rangle_{c1}|0\rangle_{c2} \rightarrow |R\rangle \otimes |0\rangle_{c1}|0\rangle_{c2}$, (f): while for $V_{dd} = -2J$, the atomic transition $|G\rangle \otimes |0\rangle_{c1}|2\rangle_{c2} \rightarrow |R\rangle \otimes |0\rangle_{c1}|0\rangle_{c2}$ is caused by absorption of two photons from c_2 .

frequency of the normal mode c_1 , while the other channel $|G\rangle \rightarrow |A\rangle \rightarrow |R\rangle$ is out of resonance and is detuned by $4J$. Therefore, under the condition $J \gg \sqrt{n_{c1}}\lambda$, we can finally obtain an effective Hamiltonian by using the time averaging approach to describe this two-photon transition process [21],

$$H_{eff} = \xi(|G\rangle\langle R|c_1^{\dagger 2} + |R\rangle\langle G|c_1^2), \quad (6)$$

where $\xi = \lambda^2/J$, and the stark shift terms $(\lambda^2/J)[(c_1^\dagger c_1 - c_2^\dagger c_2)|G\rangle\langle G| + |R\rangle\langle R|(c_1 c_1^\dagger + c_2 c_2^\dagger/3)]$ have been neglected because they are much less than the photon number dependent energy H_{st} . While if $V_{dd} = -2J$, the transition channel $|G\rangle \leftrightarrow |R\rangle$ mediated by the singlet state $|A\rangle$ is in resonance with twice the frequency of the normal mode c_2 , and the channel $|G\rangle \rightarrow |S\rangle \rightarrow |R\rangle$ related to c_1 is out of resonance. The effective Hamiltonian is then otherwise

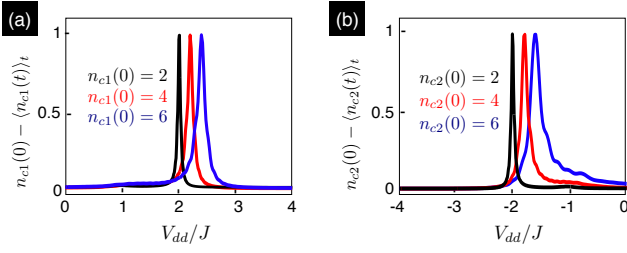


FIG. 3. (Color online) (a) Time-averaged photon absorption versus V_{dd}/J with initial system state (a) $|G\rangle \otimes |n_{c1}\rangle_{c1}|0\rangle_{c2}$ and (b) $|G\rangle \otimes |0\rangle_{c1}|n_{c2}\rangle_{c2}$ over $t \in [0, 2\pi/\sqrt{n_{c1,2}(n_{c1,2}-1)\xi}]$. The absorption centers are shifted according to the photon number dependent Stark shifts described by H_{st} . Other parameters as in Fig. 2.

given by

$$H_{eff} = \xi(|G\rangle\langle R|c_2^{\dagger 2} + |R\rangle\langle G|c_2^2). \quad (7)$$

Thus, the blockade of the double Rydberg excitations may be wrecked due to the photon hopping through two-photon absorption. (ii) Two-photon transition including H_{st} . Taking stark shift H_{st} into consider, the two-photon resonant transition may break down if $|G\rangle$ and $|R\rangle$ are shifted by different amount depending on the photon number of the normal modes. Set $\Omega = g$, this implies the two-photon resonance condition $V_{dd} = 2J + (\langle n_{c1} \rangle - 2)\lambda$ and $V_{dd} = -2J + (\langle n_{c2} \rangle - 2)\lambda$ for c_1 mode and c_2 mode, respectively, when the atoms are initially in the ground state $|g\rangle$. The energy shifts of the symmetric and anti-symmetric entangled states will slightly modify the effective two-photon coupling rate.

The coherent quantum dynamics in this atom-cavity coupled system can be read from Fig.2, in which we have shown the time-dependent population of the collective atomic states with the system initial state $|G\rangle \otimes |1\rangle_{a1}|1\rangle_{a2}$. In terms of the delocalized normal modes, the initial state of the cavity fields can be rewritten as $a_1^\dagger a_2^\dagger |0\rangle_{a1}|0\rangle_{a2} = \frac{1}{2}(c_1^\dagger + c_2^\dagger)(c_1^\dagger - c_2^\dagger)|0\rangle_{c1}|0\rangle_{c2} = (|2\rangle_{c1}|0\rangle_{c2} - |0\rangle_{c1}|2\rangle_{c2})/\sqrt{2}$. In this case, the energy shifts for $|G\rangle$ and $|R\rangle$ are both 2λ , which guarantee the two-photon resonance condition. In Fig. 2(a) and 2(d), the Rabi oscillation between $|G\rangle$ and $|R\rangle$ clearly demonstrates the photon absorption and emission processes, and the excitation of the symmetric and anti-symmetric entangled states are well suppressed. The probability for detecting $|R\rangle$ can only reach 0.5 or so in each plot because the transition channels via the intermediate state $|S\rangle$ and $|A\rangle$ are selected by the sign of the energy shift V_{dd} . In this process, the photon dynamics of the localized modes a_1 and a_2 display exactly the same behavior and remain symmetric. It means that the two localized photons are absorbed and emitted simultaneously all the time (see Fig. 2(b) and 2(e)). In contrast, the coupling to the delocalized normal modes are symmetry breaking. Either the transition between $|G\rangle \otimes |2\rangle_{c1}|0\rangle_{c2}$ and $|R\rangle \otimes |0\rangle_{c1}|0\rangle_{c2}$ with $V_{dd} = 2J$ or that between $|G\rangle \otimes |0\rangle_{c1}|2\rangle_{c2}$ and

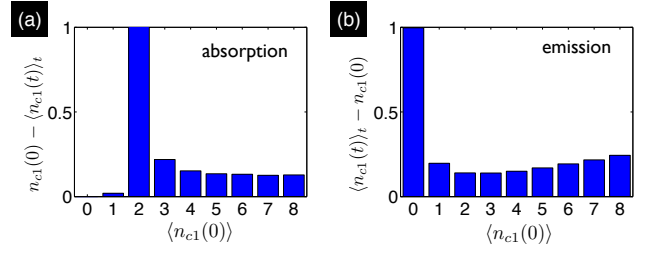


FIG. 4. (Color online) (a) Time-averaged photon absorption in $t \in [0, 2\pi/\sqrt{2}\xi]$ versus n_{c1} with initial system state $|G\rangle \otimes |n_{c1}\rangle_{c1}|0\rangle_{c2}$. (b) Time-averaged photon emission in $t \in [0, 2\pi/\sqrt{2}\xi]$ versus n_{c1} with initial system state $|R\rangle \otimes |n_{c1}\rangle_{c1}|0\rangle_{c2}$. Other parameters as in Fig. 3.

$|R\rangle \otimes |0\rangle_{c1}|0\rangle_{c2}$ with $V_{dd} = -2J$ happens. That is accompanied by the absorption and emission of two delocalized photons (Fig.2(c) and 2(f)). Note that the effective coupling strength should be revised by $\xi' = \lambda^2/(J \pm \lambda/2)$ for $V_{dd} = \pm 2J$ due to the energy shifts of $|S\rangle$ and $|A\rangle$, which leads to the slightly different time period of oscillation for $\langle n_{c1} \rangle$ and $\langle n_{c2} \rangle$. The time evolution of the system dynamics discussed above can be analytically calculated by solving the Schrödinger equation $i\hbar\dot{\psi}(t) = H_{eff}\psi(t)$. Without loss of generality, we focus on the two-photon transition with respect to the delocalized mode c_1 described by Eq. (6), from which we can obtain the quantum state of the system at time t ,

$$|\psi(t)\rangle = \frac{1}{\sqrt{2}}(C_g(t)|G\rangle \otimes |2\rangle_{c1}|0\rangle_{c2} + C_r(t)|R\rangle \otimes |0\rangle_{c1}|0\rangle_{c2}) - \frac{1}{\sqrt{2}}|G\rangle \otimes |0\rangle_{c1}|2\rangle_{c2}. \quad (8)$$

In addition, by appropriately choosing the interaction time, the system will evolve from $|G\rangle \otimes (|2\rangle_{c1}|0\rangle_{c2} - |0\rangle_{c1}|2\rangle_{c2})/\sqrt{2}$ ($|G\rangle \otimes |1\rangle_{a1}|1\rangle_{a2}$) onto $|G\rangle \otimes (|2\rangle_{c1}|0\rangle_{c2} + |0\rangle_{c1}|2\rangle_{c2})/\sqrt{2}$ ($|G\rangle \otimes (|2\rangle_{a1}|0\rangle_{a2} + |0\rangle_{a1}|2\rangle_{a2})$), which is a two-photon NOON state for localized modes.

The physical model can be further understood by looking into the time averaged photon absorption $n_{c1}(0) - \langle n_{c1}(t) \rangle_t$ ($n_{c2}(0) - \langle n_{c2}(t) \rangle_t$) as a function of the Rydberg-Rydberg interaction strength for the initial state $|G\rangle \otimes |n_{c1}\rangle_{c1}|0\rangle_{c2}$ ($|G\rangle \otimes |0\rangle_{c1}|n_{c2}\rangle_{c2}$) with varied photon number (see Fig. 3). It is found that the two-photon absorption centers are shifted according to the photon number dependent energy shifts for $|G\rangle \otimes |n_{c1}\rangle_{c1}|0\rangle_{c2}$ and $|G\rangle \otimes |0\rangle_{c1}|n_{c2}\rangle_{c2}$ that are illustrated by H_{st} . For $V_{dd} \simeq 2J$ or $V_{dd} \simeq -2J$, only when $n_{c1} = 2$ and $n_{c2} = 0$, or $n_{c1} = 0$ and $n_{c2} = 2$, the interplay between Rydberg-Rydberg interaction and photon tunneling will cause absorption of two photons from the normal modes. The resonant two-photon transition gives time-averaged photon absorption of one. For the initial state being $|G\rangle \otimes |n_{c1}\rangle_{c1}|0\rangle_{c2}$ and $n_{c1} \neq 2$, this corresponds to the dispersive interaction regime because the $|G\rangle \leftrightarrow |R\rangle$ transition is detuned by $(n_{c1} - 2)\lambda$, which is much larger than the effective $|G\rangle \leftrightarrow |R\rangle$ coupling

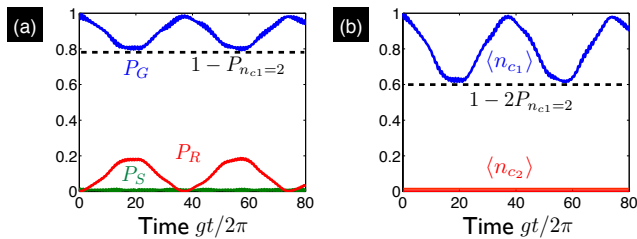


FIG. 5. (Color online) Time dependent population of the collective atomic states and mean photon number for optical normal modes c_1 and c_2 for initially the atoms in the state $|G\rangle$ and the cavity modes in the coherent states $|\alpha\rangle_{a1}|\beta\rangle_{a2} = |(\alpha + \beta)/\sqrt{2}\rangle_{c1}|(\alpha - \beta)/\sqrt{2}\rangle_{c2}$, where $\alpha = \beta = 1/\sqrt{2}$. The interaction of the atoms with cavity fields is mainly dominated by the $|G\rangle \otimes |2\rangle_{c1}|0\rangle_{c2} \rightarrow |R\rangle \otimes |0\rangle_{c1}|0\rangle_{c2}$ transition. The oscillational amplitude is limited by the probability amplitude of the component $|2\rangle_{c1}$ is $|(\alpha + \beta)/\sqrt{2}\rangle_{c1}$ expanded in Fock space. The normal mode c_2 is unpopulated during the interaction. The parameters are $\Omega = g$, $\delta = 10g$, $J = 0.998g$, and $V_{dd} = 2g$.

strength $\sqrt{n_{c1}(n_{c1} - 1)}\xi$. As shown in Fig. 4(a), the photon absorption becomes weaker and weaker as the initial photon number of c_1 mode increases. It is also interesting to study the time averaged photon emission $\langle n_{c1}(t) \rangle_t - n_{c1}(0)$ with the system initial state $|R\rangle \otimes |n_{c1}\rangle$ (see Fig. 4(b)). Here, the atoms are both initially in the Rydberg excited state. The atomic transition $|R\rangle \rightarrow |G\rangle$ regularly happens accompanied by simultaneously emitting two photons for the normal mode being in the vacuum state, giving rise to emission enhancement of the mode. For $n_{c1}(t = 0) > 1$, the normalized photon emission given by $(\langle n_{c1}(t) \rangle_t - n_{c1}(0))/n_{c1}(0)$ goes down as $n_{c1}(0)$ grows.

IV. QUANTUM NONCLASSICAL PROCESS AND QUANTUM FILTER

Now we consider the localized cavity fields that are initially in the coherent states $|\alpha\rangle_{a1}$ and $|\beta\rangle_{a2}$ respectively. The quantum state of the localized two-mode field can be rewritten as $|\alpha\rangle_{a1}|\beta\rangle_{a2} = |(\alpha + \beta)/\sqrt{2}\rangle_{c1}|(\alpha - \beta)/\sqrt{2}\rangle_{c2}$ in terms of the normal modes c_1 and c_2 , which are the coherent states of mean photon number $\langle N_{c1} \rangle = |\alpha + \beta|^2/2$ and $\langle N_{c2} \rangle = |\alpha - \beta|^2/2$. For $\alpha = \beta$, the c_2 mode is in the vacuum state. Thus, if the atoms are both in the ground state $|g\rangle$ and the Rydberg-Rydberg interaction strength is $V_{dd} = 2J$, only the transition channel $|G\rangle \rightarrow |S\rangle \rightarrow |R\rangle$ will be opened for the coupling of $|G\rangle$ with $|R\rangle$. We can then simply focus on the photon dynamics of the c_1 mode. To study the c_2 mode, we can alternatively set $\alpha = -\beta$. Without loss of generality, we will assume $\alpha = \beta$ in the following. The c_1 mode can be expanded in the Fock state representation as $|(\alpha + \beta)/\sqrt{2}\rangle_{c1} = \exp(-|\alpha + \beta|^2/2) \sum_{n=0}^{\infty} ((\alpha + \beta)/\sqrt{2})^n / \sqrt{n!} |n\rangle_{c1}$. As discussed above, the effective Hamiltonian in Eq.(6) or

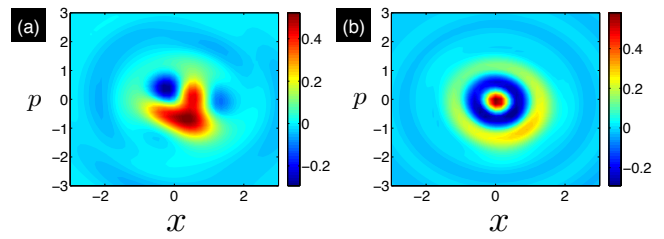


FIG. 6. (Color online) Wigner function $W(x, p)$ of the normal mode c_1 after interaction with Rydberg atoms. The initial states are: (a) $|G\rangle \otimes |\alpha = 1/\sqrt{2}\rangle_{a1}|\beta = 1/\sqrt{2}\rangle_{a2}$ and (b) $|R\rangle \otimes |\alpha = 1/\sqrt{2}\rangle_{a1}|\beta = 1/\sqrt{2}\rangle_{a2}$. Other parameters as in Fig. 5.

Eq.(7) holds only when there are two photons in c_1 mode. Otherwise, the collective atomic states $|G\rangle$ and $|R\rangle$ will be shifted by different amount and the $|G\rangle \leftrightarrow |R\rangle$ transition is thus out of resonance. This can be used for demonstration of the quantum nonclassical process [22], where a coherent state will be transformed to a nonclassical state. The coherent dynamics of the Rydberg atoms interacting with coherent cavity fields is shown in Fig. 5. The oscillation is mainly due to the interplay of $|G\rangle \otimes |0\rangle_{c1}|2\rangle_{c2}$ with $|R\rangle \otimes |0\rangle_{c1}|0\rangle_{c2}$ weakly perturbed by $|G\rangle \otimes |n\rangle_{c1}|0\rangle_{c2}$ ($n_{c1} \neq 2$). Therefore, the minimum of the atomic population P_G and the mean photon number of c_1 mode $\langle n_{c1} \rangle$ are approximately given by $(1 - P_{n_{c1}=2})$ and $(1 - 2P_{n_{c1}=2})$, respectively, with $P_{n_{c1}=2}$ the probability amplitude of $|2\rangle_{c1}$ in the expansion of coherent state in the Fock space.

Using this system, we can realize a quantum nonlinear absorption filter and the nonclassical quantum optical process defined by Rahimi-Keshari et al. [22]. For the atoms interacting with coherent cavity fields with the initial state $|G\rangle \otimes |\sqrt{2}\alpha\rangle_{c1}|0\rangle_{c2}$, the measurement of the atoms in the state $|G\rangle$ at $t = \pi/2\sqrt{2}\xi$ will collapse the normal mode c_1 into a nonclassical quantum state finally by removing the component Fock state $|2\rangle$ from coherent c_1 mode. Note that the density operator of an arbitrary field state can be written as $\rho = \int P(\alpha)|\alpha\rangle\langle\alpha|d^2\alpha$ by means of a diagonal representation in terms of the coherent states, and the probability distribution of the photon-number states in ρ is given by $p(n) = \int P(\alpha)|\langle n|\alpha\rangle|^2 d^2\alpha$. Because $|\langle n|\alpha\rangle|^2 > 0$, $p(n)$ can not be zero for any n when $P(\alpha)$ is a true probability density. Then, any field state for which $p(n) = 0$ has no classical analog and deserves special attention [23]. Therefore, the state of the normal mode c_1 with $p(n = 2) = 0$ is purely quantum mechanical. The Wigner function for such kind of nonclassical states is shown in Fig.6(a), from which we clearly see the negative value close to the origin demonstrating its nonclassical nature. The component Fock state $|2\rangle_{c1}$ has been absorbed by the atoms being excited to $|R\rangle$. It corresponds to a quantum filter for a special photon number state that has been realized with linear optics based on multi-photon interference and measurement induced amplitude nonlinearity [24, 25]. On the other hand, while

the atoms initially in the collective state $|R\rangle$ interact with the coherent fields, ideally, the measurement of the atoms in the collective state $|G\rangle$ will collapse the normal mode c_1 into the Fock state $|2\rangle_{c1}$, which is weakly influenced by the components of the other Fock states. The Wigner function of the normal mode c_1 after atomic measurement is shown in Fig. 6(b), which predicates a Fock state $|2\rangle_{c1}$ in despite of tiny distortion. This can probably be used for realization of two-photon source, in particular, for the cavity fields initially being in the vacuum states. Although we assumed the cavity fields are initially in the coherent states, the characteristics of current model are applicable to tailor different quantum states of light, such like thermal fields in coupled cavities.

V. THE EXPERIMENTAL REALIZATION

The schematic setup and the theoretical model studied in this paper may be experimentally realized with quantum optical devices such as coupled toroid microcavities [26] or waveguide-coupled Fabry-Perot cavities [27, 28]. We assumed that each cavity contains only a single optical mode. The single mode assumption is valid when the cavity coupling J is small compared with the free spectral range (FSR) of the each uncoupled cavity. With toroid microcavities, the coupling of the initially uncoupled whispering-gallery modes can be realized via control of the air gap between the microtoroids, and therefore the overlap of evanescent fields. This has been demonstrated recently by Grudinin et al. [26]. The cavity coupling J can be tuned ranging from 5MHz to 5GHz, which is much less than the FSR that is on the order of several hundred GHz [29]. On the other hand, the optical modes can be made degenerate in frequency by thermal control of the microtoroids [26]. Therefore, only two modes (one from each microtoroid) contribute to the coupled system. The atoms coupled to the resonators' evanescent field can then interact through dipole-dipole or van der Waals interaction [30]. For waveguide-coupled Fabry-Perot cavities, the cavity coupling of the strength $J \sim 2\pi \times 50\text{MHz}$ and the free spectral range beyond $2\pi \times 1\text{GHz}$ are achievable [27]. Therefore, the single mode cavity assumption proposed here should be reasonable. In addition, the waveguide-coupled Fabry-Perot cavities setup was studied in detail for its potential application in constructing a Jaynes-Cumming lattice and simulating the quantum dynamics of a spin chain [27]. The microcavities are open in the transverse direction and the longitudinal cavity axes are separated by several microns, giving access to lasers that excite the atoms to the Rydberg state. Assuming that each atom is at the center of its cavity, the Rydberg coupling then depends on the transverse distance between the microcavities. Therefore, the Rydberg-Rydberg interaction should in principle be the same as the Rydberg atoms in vacuum.

For experimental demonstration of the two-photon absorption and emission, the parameter ξ of the effective

Hamiltonian should be much larger than effective decoherence rates via the photons and the excited states. Set $\Omega = g$, $\delta = 10g$, and $J = g$, then we have $\lambda = \Omega g/\delta = 0.1g$, $\xi = \lambda^2/J = 0.01g$, and the time needed for preparing nonclassical states shown in Fig. 6 is $t = \pi/2\sqrt{2}\xi \simeq 1.11 \times 10^2 g^{-1}$. Since the intermediate state $|e\rangle$ is off-resonantly coupled with the ground state $|g\rangle$ and the Rydberg state $|r\rangle$, the effective decay rate for $|e\rangle$ is $\gamma_e = (g^2/\delta^2 + \Omega^2/\delta^2)\gamma$ for $\delta \gg \Omega, g, \gamma$, where γ is the spontaneous emission rate. The Rydberg state with principal quantum number $n = 70$ has a spontaneous decay rate $\gamma_r = 2\pi \times 0.55\text{kHz}$ that is much smaller than γ . The cavity decay rate should fulfill the condition $\kappa \ll \xi \sim 0.01J$, which implies the photons fast tunnel to next cavity before decay into free space. These decoherence sources will induce intrinsic errors for the implementation. On the other hand, the Rydberg-Rydberg interaction arises from the intrinsic Förster interaction, which can lead to the energy shift V_{dd} approximating to 200MHz with the interatomic distance around $7\mu\text{m}$ [8]. The sign of the energy shift is determined by the sign of Förster defects correlated with the selected transition channels [20]. The parameter regime above can be achieved with the micro-cavities, where atom-cavity interacting system with the cooperativity factor as high as $C = g^2/2\kappa\gamma \sim 10^5$ is predicted to be available [31]. The micro-cavities with the size tens of μm can be coupled via the overlap of their evanescent fields. Set $\kappa \sim 10^{-3}g$ and $\gamma \sim 10^{-3}g$, the errors of the prepared nonclassical state due to decoherence approximates to $E \simeq (\gamma_e + \gamma_r + \kappa)t \simeq 0.12$. Without seeing a quantum jump from the coupled cavities, the dissipative dynamics of the system can be described by the non-Hermitian Hamiltonian $H_{NH} = H_I - i\kappa/2(a_1^\dagger a_1 + a_2^\dagger a_2)$, using which we find that the successful probability of the current proposal decreases according to the exponential factor $e^{-\bar{n}_c \kappa t}$ with \bar{n}_c the mean photon number in coupled cavities, while the Wigner function for the prepared state is only slightly changed. To improve the fidelity, an atomic ensemble acting as a two-level "superatom" can be placed inside the cavities, instead of a single Rydberg atom [32].

VI. CONCLUSION

In conclusion, we have studied the interaction between Rydberg atoms and the normal modes in coupled cavities. The dispersive atom-cavity interaction results in nonlinear electronic-level shifts depending on the photon-number of the normal modes. The Rydberg atoms can simultaneously absorb (emit) two photons from (into) one of the normal modes relying on the sign of the Rydberg-Rydberg interaction induced energy shift. There is only one transition channel that is in two-photon resonance, which can be used for generation of nonclassical states of light and realization of a quantum filter. The physical realization of this scheme can be realized with coupled micro-cavities, however, the alternative candidates

of experimental setup include ultrahigh-Q coupled nanocavity based on photonic crystals [33] and superconducting microwave devices [18, 19]. This scheme promises a new avenue for manipulation of quantum state of light and realization of nonclassical quantum optical process.

ACKNOWLEDGMENTS

This work was supported by the Major State Basic Research Development Program of China under grant no.

2012CB921601, the National Natural Science Foundation of China under grant no. 11247283, no. 11305037, and no. 11374054, the Natural Science Foundation of Fujian Province under grant no. 2013J01012, and the fund from Fuzhou University.

-
- [1] H. J. Kimble, Proceedings of the Les Houches Summer School, Session LIII, edited by J. Dalibard, J. M. Raimond, and J. Zinn-Justin (North-Holland, Amsterdam, 1992).
- [2] S. Haroche and J. M. Raimond, *Exploring the Quantum: Atoms, Cavities, and Photons* (Oxford University Press, Oxford, 2006).
- [3] Y. Yamamoto and A. Imamoglu, *Mesoscopic Quantum Optics* (John Wiley and Sons Inc., 1999).
- [4] V. Bartzis and N. Nayak, *J. Opt. Soc. Am. B* **8**, 1779 (1991).
- [5] C. K. Hong and L. Mandel, *Phys. Rev. Lett.* **56**, 58 (1986).
- [6] P. G. Kwiat, K. Mattle, H. Weinfurter, A. Zeilinger, A. V. Sergienko, and Y. Shih, *Phys. Rev. Lett.* **75**, 4337 (1995).
- [7] C. Simon and J.-P. Poizat, *Phys. Rev. Lett.* **94**, 030502 (2005).
- [8] C. Guerlin, E. Brion, T. Esslinger, and K. Mølmer, *Phys. Rev. A* **82**, 053832 (2010).
- [9] X.-F. Zhang, Q. Sun, Y.-C. Wen, W.-M. Liu, S. Eggert, and A.-C. Ji, *Phys. Rev. Lett.* **110**, 090402 (2013).
- [10] J.-F. Huang, J.-Q. Liao, and C. P. Sun, *Phys. Rev. A* **87**, 023822 (2013).
- [11] M. Saffman, T. G. Walker, and K. Mølmer, *Rev. Mod. Phys.* **82**, 2313 (2010).
- [12] V. Parigi, E. Bimbard, J. Stanojevic, A. J. Hilliard, F. Nogueira, R. Tualle-Broui, A. Ourjoumtsev, and P. Grangier, *Phys. Rev. Lett.* **109**, 233602 (2012).
- [13] T. Peyronel, O. Firstenberg, Q.-Y. Liang, S. Hofferberth, A. V. Gorshkov, T. Pohl, M. D. Lukin, and V. Vuletic, *Nature(London)* **488**, 57 (2012).
- [14] C. D. Ogden, E. K. Irish, and M. S. Kim, *Phys. Rev. A* **78**, 063805 (2008).
- [15] Z. B. Yang, H. Z. Wu, Y. Xia, and S. B. Zheng, *Eur. Phys. J. D* **61**, 737 (2011).
- [16] M. J. Hartmann, F. G. S. L. Brandao, and M. B. Plenio, *Nat. Phys.* **2**, 849 (2006).
- [17] G. Chen, T. H. Stievater, E. T. Batteh, X. Li, D. G. Steel, D. Gammon, D. S. Katzer, D. Park, and L. J. Sham, *Phys. Rev. Lett.* **88**, 117901 (2002).
- [18] D. Petrosyan and M. Fleischhauer, *Phys. Rev. Lett.* **100**, 170501 (2008).
- [19] S. D. Hogan, J. A. Agner, F. Merkt, T. Thiele, S. Filipp, and A. Wallraff, *Phys. Rev. Lett.* **108**, 063004 (2012).
- [20] T. G. Walker and M. Saffman, *Phys. Rev. A* **77**, 032723 (2008).
- [21] D. F. V. James, *Fortschr. Phys.* **48**, 823 (2000).
- [22] S. Rahimi-Keshari, T. Kiesel, W. Vogel, S. Grandi, A. Zavatta, and M. Bellini, *Phys. Rev. Lett.* **110**, 160401 (2013).
- [23] L. Mandel and E. Wolf, *Optical Coherence and Quantum Optics* (Cambridge University Press, New York, 1995).
- [24] K. Sanaka, K. J. Resch, and A. Zeilinger, *Phys. Rev. Lett.* **96**, 083601 (2006).
- [25] T. J. Bartley, G. Donati, J. B. Spring, X.-M. Jin, M. Barbieri, A. Datta, B. J. Smith, and I. A. Walmsley, *Phys. Rev. A* **86**, 043820 (2012).
- [26] I. S. Grudinin, H. Lee, O. Painter, and K. J. Vahala, *Phys. Rev. Lett.* **104**, 083901 (2010).
- [27] G. Lepert, M. Trupke, M. J. Hartmann, M. B. Plenio, and E. A. Hinds, *New J. Phys.* **13**, 113002 (2011).
- [28] G. Lepert, E. A. Hinds, H. L. Rogers, J. C. Gates, and P. G. R. Smith, arXiv:1304.7013.
- [29] S. M. Spillane, PhD thesis, California Institute of Technology, 2004.
- [30] T. Aoki, B. Dayan, E. Wilcut, W. P. Bowen, A. S. Parkins, T. J. Kippenberg, K. J. Vahala, and H. J. Kimble, *Nature(London)* **443**, 671 (2006).
- [31] S. M. Spillane, T. J. Kippenberg, K. J. Vahala, K. W. Goh, E. Wilcut, and H. J. Kimble, *Phys. Rev. A* **71**, 013817 (2005).
- [32] V. Vuletic, *Nat. Phys.* **2**, 801 (2006).
- [33] M. Notomi, E. Kuramochi, and T. Tanabe, *Nat. Photon.* **2**, 741 (2008).